ADVANCED ENERGY MATERIALS
www.advenergymat.de

Kinetics Dominated, Interface Targeted Rapid Heating for Battery Material Rejuvenation

Hao Zhang, Yaduo Song, Jiale Zhao, Zhiheng Cheng, Jinming Guo, Minglei Cao, Haijun Yu, Hao Wang, Long Qie, Lixia Yuan, Yonggang Yao, and Yunhui Huang**

The ambitious pursuit of carbon neutrality underscores the pressing demand for closed-loop recycling of lithium-ion batteries (LIBs), amid escalating production and disposal challenges. Direct battery material recycling, emphasizing the rejuvenation of degraded materials, stands out as an environmentally benign alternative to conventional pyro- and hydro-metallurgical processes that are intrinsically destructive. In addition, given the surface, interface, and interphase as the major failure mechanisms in degraded materials, rapid heating technology (RHT) emerges as a promising direct recycling method, harnessing its distinctive kinetics and thermodynamics to trigger highly time- and energy-efficient, precisely defect- and interface-targeted approach to revitalize degraded materials. This review summarizes recent advancements in RHT-based LIB recycling strategies, focusing on active materials recovery, efficient regeneration, and reutilization, with emphasis on expedited kinetics and locally confined chemical reactions at interfaces. It also outlines the perspectives and future directions by emphasizing the need for re-manufactured materials to meet increasing application demands. This comprehensive review aims to guide the recycling and upcycling of spent LIBs toward a green and sustainable battery economy.

1. Introduction

Lithium-ion batteries (LIBs) have garnered widespread adoption in both industrial and daily life applications, serving as energy storage systems and power sources for electric vehicles.[1] Their appeal stems from their exceptional attributes: high energy density, lengthy cycling lifespan, minimal self-discharge rates, and the absence of memory effects. Nevertheless, as LIB production ramps up and their usage proliferates, challenges have emerged concerning the accessibility and price volatility of raw materials, as well as the disposal of spent LIBs.[2–4] These issues underscore the urgent need for closed-loop mass production to sustain the battery economy.

Recently, direct recycling techniques, which focus on rejuvenating degraded materials, have emerged as advantageous alternatives to hydrometallurgical and pyrometallurgical recycling methods.[5,6] Direct recycling boasts lower energy consumption, reduced carbon emissions, and heightened profitability, making it a compelling strategy for promoting environmental sustainability.[7,8] To devise effective direct recycling strategies, a comprehensive understanding of the failure mechanisms of degraded materials is paramount.[9–12] Given that battery performance hinges crucially on the efficient transfer and storage of lithium ions,[13] the failure mechanisms can be spatially categorized into three primary aspects: 1) the surface model, where electrochemical reactions at the solid-liquid interface lead to degradation of the active material's surface, manifesting as thick and porous solid electrolyte interface (SEI) layers,[14] rock salt phase formation,[15] oxygen vacancies, and so on; 2) the interface model, where surface degradation weakens and damages effective electron conduction and physical connections between particles and between particles and current collectors; and 3) the bulk defects model, representing lithium loss,[16] cation mixing and so on. Thus, the key points of direct recycling are targeting these locally degraded structures, harnessing their potential, and reconstructing them to restore functionality.

In response to these diverse failure mechanisms, characterized by defects and interfaces with reduced activation energies (**Figure 1A**), researchers have proposed a myriad

H. Zhang, Y. Song, J. Zhao, Z. Cheng, L. Qie, L. Yuan, Y. Yao, Y. Huang
State Key Laboratory of Materials Processing and Die & Mould Technology
School of Materials Science and Engineering
Huazhong University of Science and Technology
Wuhan 430074, China
E-mail: yaoyg@hust.edu.cn; huangyh@hust.edu.cn
H. Zhang, J. Guo
School of Materials Science and Engineering
Hubei University
Wuhan 430062, China
M. Cao
Hubei Key Laboratory of Energy Storage and Power Battery
School of Mathematics
Physics and Optoelectronic Engineering
Hubei University of Automotive Technology
Shiyan 442002, China
H. Yu, H. Wang
Yichang Brunp Recycling Technology Co., Ltd
Yichang 443000, China

The ORCID identification number(s) for the author(s) of this article can be found under https://doi.org/10.1002/aenm.202404838

DOI: 10.1002/aenm.202404838

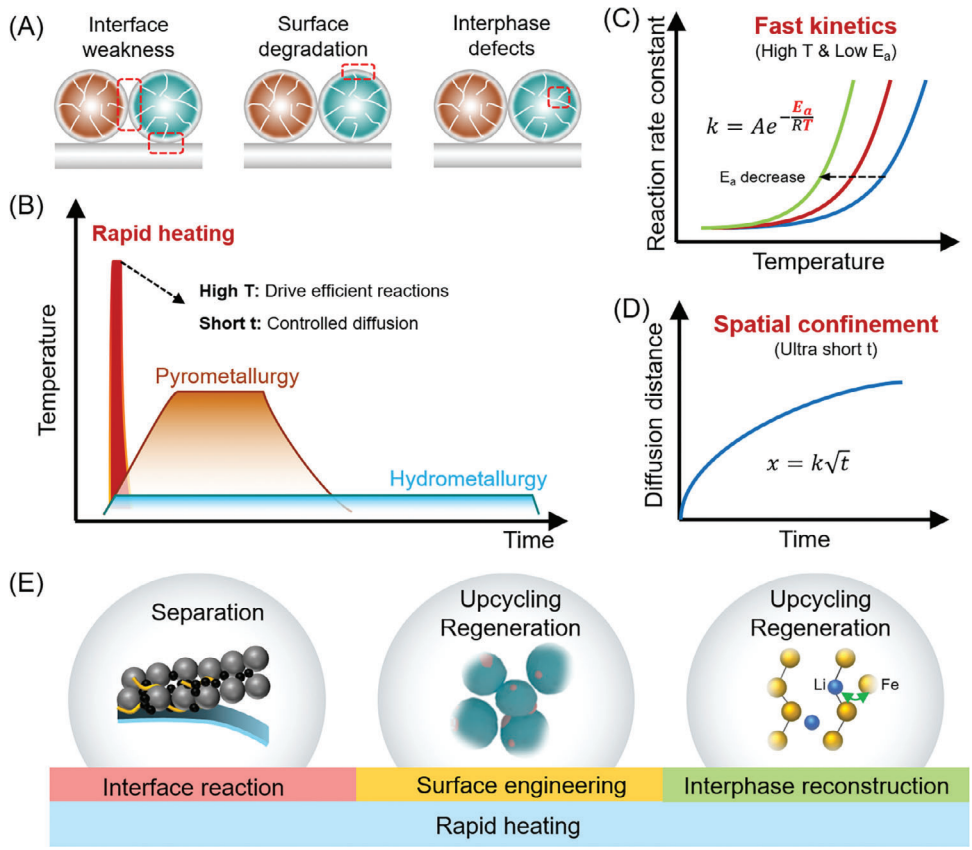

Figure 1. A) Spatial distribution of failure mechanisms of spent battery materials. B) The characteristics and advancements of RHT compared to traditional pyro- and hydro-metallurgy. C) Fast reaction kinetics at high temperature and low activation energy according to the Arrhenius equation. D) Spatial confinement of atomic diffusion within a short time period. E) Applications of RHT for the rejuvenation of spent battery materials including separation, regeneration, and upcycling (Reproduced with permission.[20] Copyright 2023, American Chemical Society.).

of recycling strategies, including the low eutectic solvent method, hydrothermal method,[17] traditional solid-phase sintering method,[18] and rapid high-temperature method.[19–21] Among the diverse recycling methods, rapid heating manufacturing, which has found widespread application in energy and environmental sectors, has garnered significant attention owing to its unique attributes.[22–24] As shown in Figure 1B, rapid heating technology (RHT) boasts extremely high temperatures combined with ultrashort duration times, thus creating a kinetics-dominated and thermodynamically nonequilibrium environment.[25–27] These features mitigate side reactions and minimize thermal budgets.[28] Furthermore, the elevated temperatures drive reactions efficiently. According to the Arrhenius equation (Figure 1C), the reaction rate constant (k) is significantly influenced by both temperature (T) and activation energy (E_a). The "T effect" describes how an increase in temperature augments the average kinetic energy of reactant molecules, fostering a greater proportion with sufficient energy to surpass reaction energy barriers, thereby accelerating the reaction rate. Conversely, for a fixed temperature, lowering the reaction energy barriers via the "E_a effect" also expedites reactions due to a lower activation energy penalty, enhancing the reaction rate constant and fostering swift reactions during subsequent regeneration and remanufacturing processes.

In contrast to traditional heating methods, which involve extended heating times of several hours and gradual heating/cooling rates (5–10 °C min^{-1}), RHT is characterized by rapid heating/cooling rates (up to 10^4 °C s^{-1}) and ultra-short, millisecond-level precisely controllable heating durations. This enables precisely spatial control over defects and interface reactions through limited diffusion distance of atoms (Figure 1D),[29] which is not only advantageous for achieving metastable phases and kinetic intermediates while preventing side reactions, but also markedly improves energy and time efficiency. As such, RHT emerges as a promising approach for direct recycling of spent batteries, leveraging the targeted manipulation of thermodynamic and kinetic processes.[30] This innovative method boasts advantages that include significantly reduced energy and raw material inputs, lower carbon emissions, and minimized environmental impacts, thereby enhancing the sustainability of battery recycling practices. Based on these remarkable advantages, numerous exceptional studies have been published, encompassing active material separation,[31] regeneration,[19,20] and upgraded remanufacturing[32] (Figure 1E).

Despite this progress, a gap remains in reviews that systematically consolidate and generalize these prior efforts. In light of the escalating interest and rapid advancements in RHT for spent battery recycling, our objective is twofold: first, to introduce the

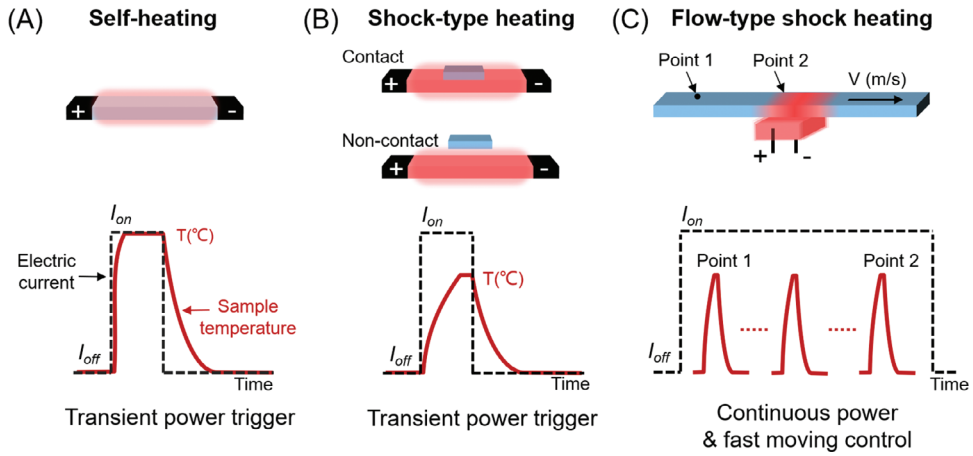

Figure 2. Illustrations and the corresponding relationships between power supply and temperature of samples for A) self-heating, B) shock-type heating, and C) flow-type shock heating.

various rapid thermal treatment methodologies and, second, to comprehensively summarize their pivotal achievements in material recovery, regeneration, and reutilization, with a focus on expedited kinetics and localized chemical reactions. Given that spent materials often stem from products 5–8 years old, remanufactured materials must keep pace with evolving application demands. Thus, when addressing practical recycling scenarios, we also delve into the perspectives and future trajectories of the rapid heating strategy. We envision that this review will serve as a guideline for the recycling and upcycling of spent LIBs through the rapid heating approach, featuring highly time- and energy-efficient and precisely defect- and interface-targeted, toward a green and sustainable battery economy.

2. Manners to Trigger Rapid Heating

The rapid high temperature is essentially triggered by an ultrahigh energy input within a short time and can be achieved through Joule heating, microwave,[33] laser irradiation,[34] or induction heating.[35,36] Among them, rapid heating induced by Joule heating is widely developed for battery recycling, due to its low cost, facile controllability, and easy scalability. Therefore, the principles of rapid heating triggered by Joule heating are introduced as examples. RHT in this review is referred to various names reported in the literatures, including transient heating,[23] ultra-fast high-temperature sintering,[37] flash Joule heating,[38,39] carbothermal shock,[40] high-temperature shock,[19,26] and shock-type heating.[31,41] RHT can be categorized based on the heating method and the control of heat treatment time into self-heating, shock-type heating, and flow-type shock heating (**Figure 2**).

1) **Self-heating** refers to the process of passing an electric current through conductive samples to generate high temperatures. Due to the self-heating effect of the samples, this method offers high energy efficiency with a rapid temperature rise rate and can achieve temperatures as high as 3000 °C in carbon materials. However, since it requires the sample to be conductive, this method is more suitable for conductive carbon-based materials, such as spent graphite. James et al. reported that in a flash Joule heating process, amorphous conductive carbon powders were lightly compressed inside a quartz or ceramic tube between two electrodes, and high-voltage electric discharge from a capacitor bank brought the carbon source to temperatures higher than 3000 K in less than 100 ms, effectively converting the amorphous carbon into turbostratic flash graphene.[42] This method allows inexpensive carbon sources, such as coal, petroleum coke, biochar, carbon black, discarded food, rubber tires, and mixed plastic waste,[43] to obtain gram-scale quantities of graphene in less than one second. In contrast to the powder mixture approach, Lu et al. directly applyed electricity to a composite film consisting of discarded photovoltaic-grade silicon and graphene oxide, resulting in a high-performance binder-free silicon nanowire/graphene composite anode.[44] For nonconductive battery materials such as lithium iron phosphate (LFP) and lithium nickel cobalt manganese oxide (NCM), they can be mixed with a certain amount of conductive carbon to achieve self-heating by electric current. For example, the black mass (a mixture of spent cathode and anode), was heated to >2100 K within seconds through a flash heating strategy.[45] Compared to the graphite and conductive carbon in the mixture, the cathode particles and SEI layer are more resistive and experience a larger power dissipation as anticipated by Joule's law. These local hotspots allow effective Joule heating to activate the black mass, leading to the improvement of leachability.
2) **Shock-type heating** realizes rapid heating treatment of the sample by contact or noncontact heat transfer from a nearby high-temperature source (such as carbon cloth, carbon felt, etc.). This method applies to both conductive and nonconductive materials as the high-temperature heating source is independent of the processing materials. For example, Yin et al reported a ultrafast repair method for regenerating spent $LiCoO_2$ cathodes within seconds through a sandwish-like heating configuration, where the spent $LiCoO_2$ powders were positioned between two high-temperature heaters.[20] However, due to the occurrence of thermal resistance, the sample's temperature lags and is lower than the heat source temperature, and its energy utilization efficiency and temperature rise rate are lower than those of self-heating.

3) The above two methods are all batch-to-batch heating solutions, while **flow-type shock heating** can achieve continuous processing of samples, which is easy to scale up and is compatible with existing industrial roll-to-roll production. Taking graphite anode scrap as an example, Zhang et al. have successfully achieved an automated separation of graphite from copper foil using a flow-type shock heating (rolled-over heating) setup.[31] By adjusting the transmission speed, the temperature of the heat source, and the heating zone, the thermal history of the samples is controlled. Among them, the heat treatment temperature is directly proportional to the heat source temperature and inversely proportional to the sample movement speed; the heat treatment time is directly proportional to the length of the heating zone and inversely proportional to the sample movement speed. It is worth noting that by expanding the number of heat sources, continuous but independently controllable multistep shock heating can be achieved, which is conducive to the high-capacity preparation of samples requiring complex treatments.

3. Direct Recycling Through Rapid High-Temperature Heating

Direct recycling of spent LIBs has garnered significant attention due to its innovative materials regeneration strategy, which involves directly converting degraded materials into new ones without breaking down their structures.[46] Unlike the element recycling strategy used in pyro- and hydro-metallurgical methods, direct recycling streamlines the resource reuse process, offering substantial advantages in terms of eco-friendliness, energy efficiency, and profitability. The direct recycling process generally consists of 1) battery disassembly, 2) active materials recovery, and 3) materials regeneration or upcycling.[8] Battery disassembly aims to collect the battery case, separator, electrolyte, cathode, and anode, which primarily depends on the advancement of automated disassembly equipment.[6,7] Materials recovery for cathode and anode electrodes focuses on obtaining active materials with low impurity content, laying the foundation for the subsequent structure and performance recovery of active materials (materials regeneration or upcycling).[47] Given the value of active materials, this review primarily discusses the application of RHT on the recycling and reuse of active materials and offers a perspective on the recycling of separators, electrolytes, and current collectors through the RHT method at the end of the review.

3.1. Active Materials Separation

In direct recycling, obtaining the active materials requires first of all efficient separation from the current collectors, which is difficult because of the vigorous binder and roll-compacted dense electrode.[48] Importantly, such separation determines the quality of collected active materials (such as high purity, less damage of phase and structure) and then affects further the easiness of regeneration strategies,[49–51] contributing significantly to the complexity and cost of the entire recycling process.[52,53] However, the commercial black mass obtained through mechanical crushing and screening methods always has a low materials recovery efficiency and contains a huge number of impurities (e.g., metal, graphite).[54] Although various strategies have been developed to date for the effective separation of active materials (e.g., tube furnace annealing,[55] electrochemical separations,[56] ultrasonic-assisted acid scrubbing,[57,58] low-temperature molten salt methods[48]), their environmental and economic benefits and scalability still cannot meet the requirements of industrialization.

In contrast, RHT is a facile, efficient, sustainable method for active materials recovery. For example, Zhang et al. achieved a high materials recovery ratio (**Figure 3B**) through RHT (e.g., continuously flow-type shock heating of 1500 °C, ≈5 m min^{-1}, Figure 3A).[31] The temperature of 1500 °C is much higher than the decomposition temperature of various binders, for example, CMC (250 °C), SBR (350 °C), and PVDF (320 °C), inducing effectively decomposition of binders lying at the interface between graphite particles and between graphite and copper foils. Meanwhile, the separated current collector foils kept an intact structure because of the ultrashort heating time, leading to a high purity of collected active materials. Especially, the Al contents of the cathode materials separated by RHT were ≈40 times lower than the commercial black mass (Figure 3C). Besides, the separated active cathode materials maintained their original phase structure, indicating that the ultra-short calcination time should contribute to the suppression of atomic diffusion and bring minimum impact to their structures. Efficient separation of spent graphite from the copper foil can also be acquired through the quick volatilization of binder and electrolyte in the microwave field (Figure 3D).[59] Notably, the residual lithium in the waste graphite still remained after the separation and could be recovered as Li_2CO_3 with a purity of 98.1% by H_2O leaching under the CO_2 atmosphere. As shown in Figure 3E, the cycling performance of the regenerated graphite at 0.5 C is also compared with the commercial one.

3.2. Active Materials Regeneration

Regeneration of the recovered active materials is essential for direct recycling.[60] To restore the structure and performance of degraded active materials, it is crucial to understand their failure/degradation mechanism.[61,62] During the charge and discharge processes of lithium-ion batteries, electrochemical reactions mainly occur at the solid-liquid interface, leading to degradation primarily at the surface and subsurface regions of the active materials, while the internal structure typically remains intact. For example, in oxide cathode materials, degradation might be caused by lithium loss,[63] particle fracture,[64] cation mixing (such as lithium-iron or lithium-nickel), or localized phase transitions.[65] For graphite anodes, degradation could be due to solvent intercalation exfoliation, lithium dendrite formation, or thickening of the SEI layer.[66] Therefore, the structural restoration of degraded active materials mainly involves localized reactions at the surface or subsurface regions.[67] Rapid high-temperature regeneration technology, which promotes rapid chemical reactions at high temperatures while controlling long-range diffusion in a short time, is advantageous for precisely repairing surface or subsurface damage to materials. This approach helps restore the electrochemical performances of active materials and provides a new strategy for the rapid, precise, and environmentally friendly regeneration of degraded active materials.

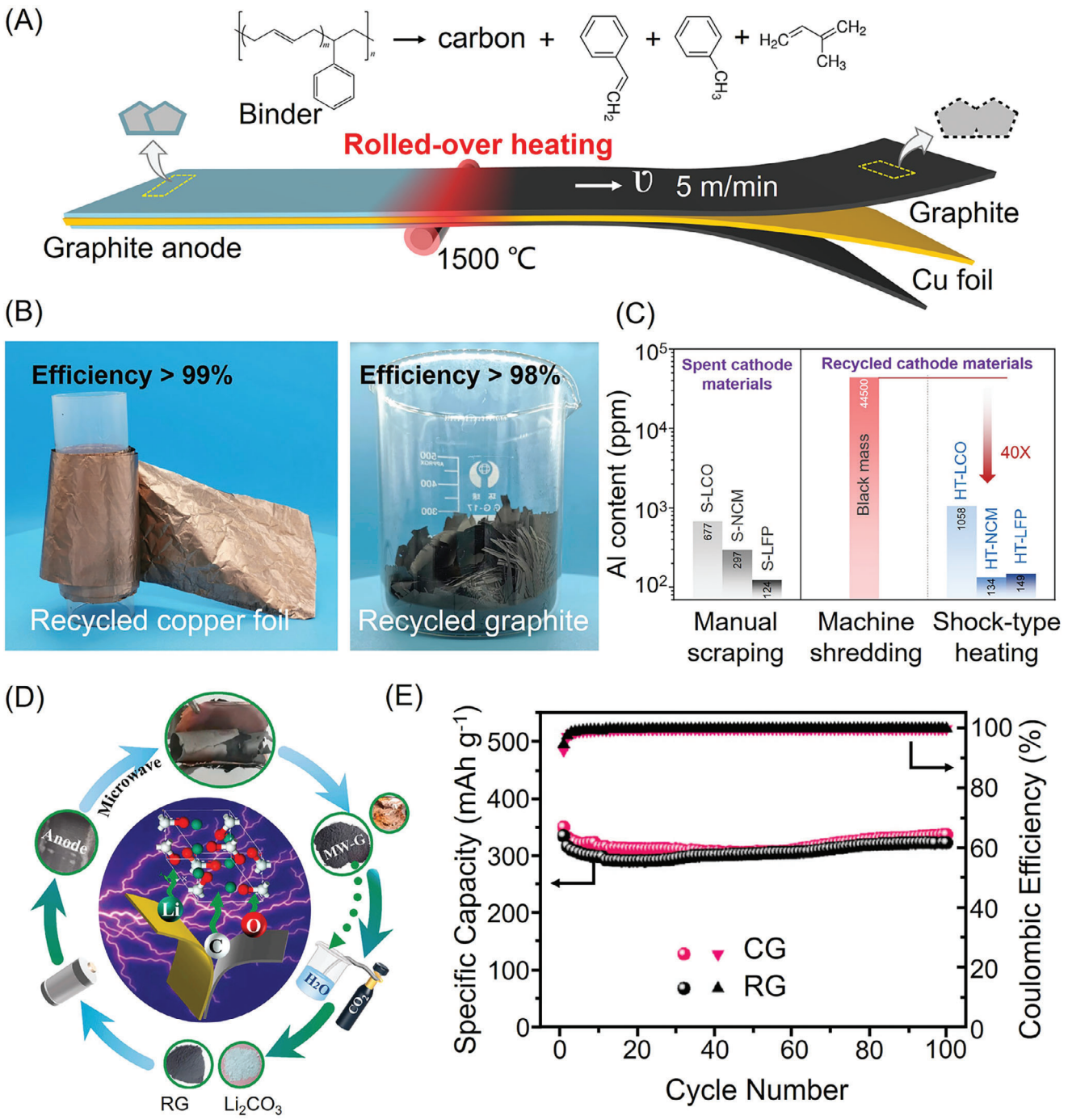

Figure 3. The separation of active materials from current collectors. A) Schematic of the separation of spent graphite from copper foils via rolled-over heating (flow-type shock heating), B) pictures of the collected copper foil and graphite, and C) the content of Al impurity in various cathode materials (Reproduced with permission.[31] Copyright 2023, The Royal Society of Chemistry.). D) Flowchart of recycling of spent anode via microwave method and E) the cycle performance of the regenerated graphite (Reproduced with permission.[59] Copyright 2021, Elsevier).

3.2.1. Surface Engineering

The SEI (or cathode electrolyte interface) coated on the active materials is crucial to their electrochemical performances. In terms of the graphite anodes, the SEI, which forms spontaneously during the charging process of LIBs, is composed of a mixture of organic and inorganic components (including $ROCO_2Li$, ROLi, LiF, etc.) and directly impacts the electrochemical performances of the battery, such as initial Coulombic efficiency, rate capability, and stability.[68,69] This makes the SEI critical for the energy density and long-term cycling of LIBs. As the charge–discharge cycling number of LIBs increases, the SEI on the

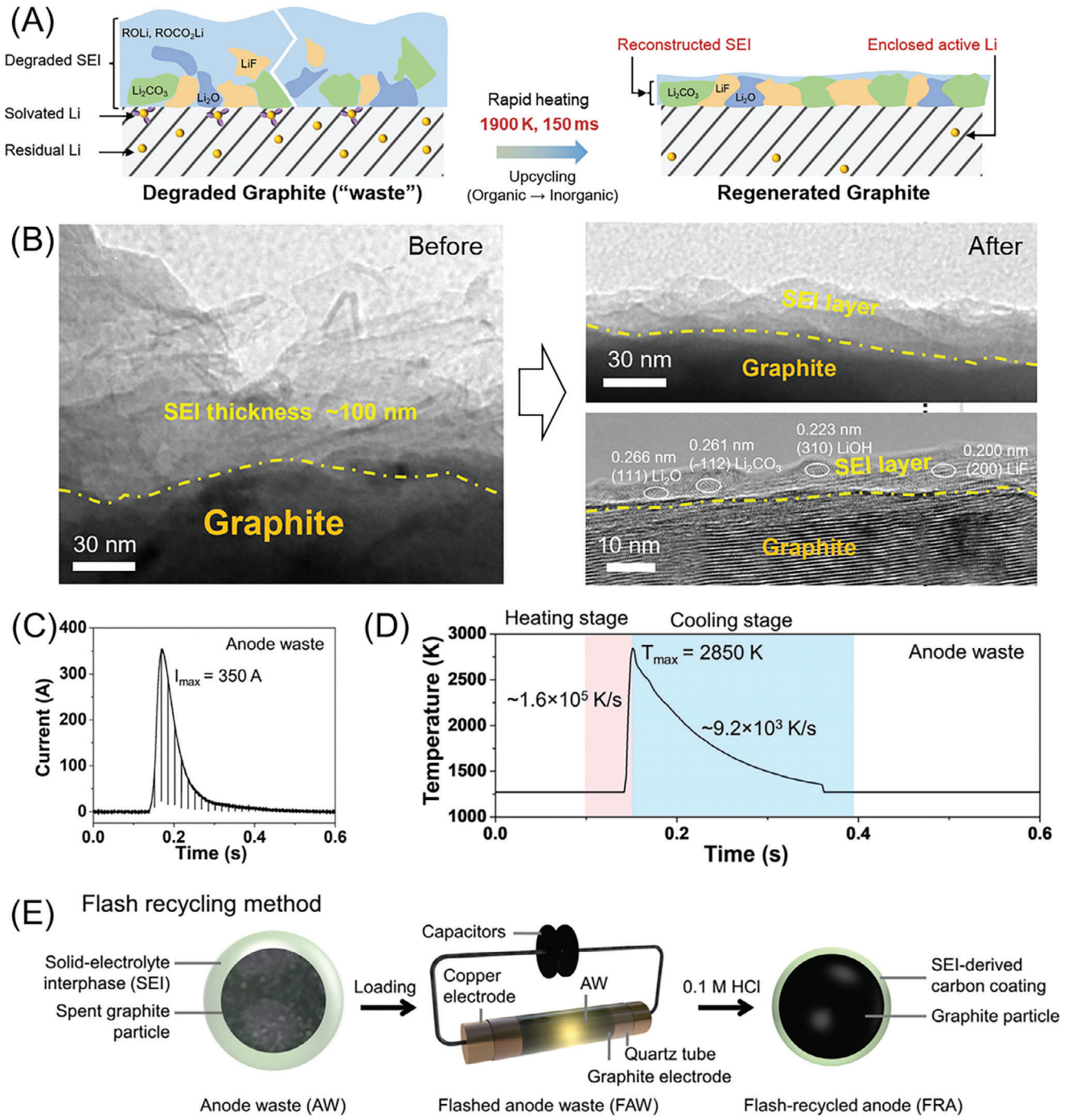

Figure 4. SEI engineering. A) Schematic diagram of SEI reconstruction on the graphite surface and B) TEM images of SEI before and after treatment (Reproduced with permission.[73] Copyright 2024, Wiley). C) Current-time curve, D) temperature-time curve during the Joule heating treatment, and E) procedures of the flash recycling method (Reproduced with permission.[74] Copyright 2023, Wiley).

graphite surface gradually becomes thick and fluffy, resulting in a continuous reduction in reversible lithium and slow diffusion kinetics of lithium ions at the negative electrode, which is an important factor in the decline of the electrochemical performances of the graphite negative electrode.[70,71] Therefore, the reconstruction and regeneration of the surface SEI is one of the important ways to restore the electrochemical performances of the degraded graphite.[72]

Ji et al. successfully regenerated the degraded graphite anode into upgraded one through the SEI reconstruction based on RHT (1900 K, 150 ms, as shown in **Figure 4A**).[73] In the approach, the fast heating instantly converted the loose organic/inorganic

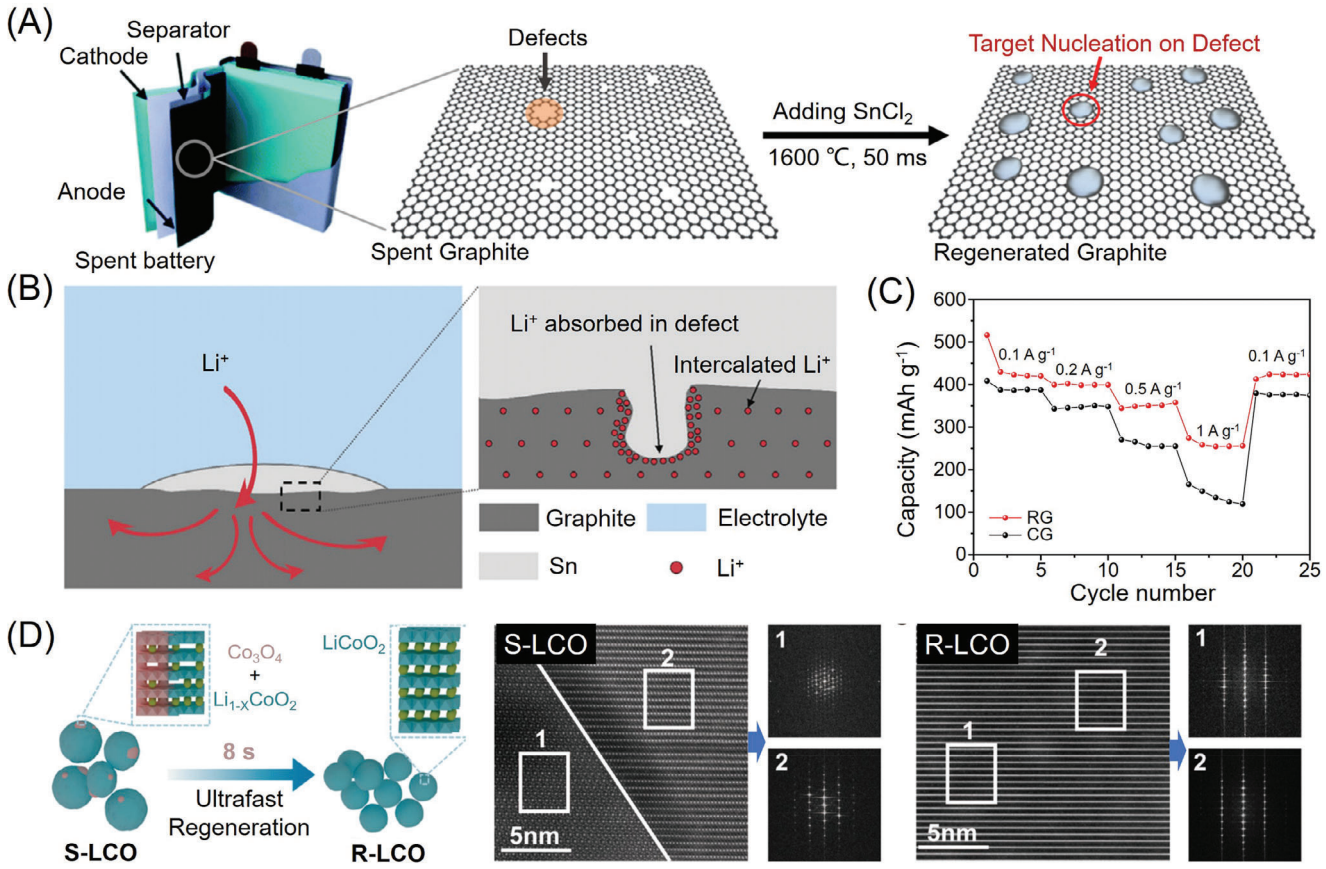

Figure 5. Surface reparation. A) Schematic of targeted regeneration and upcycling of spent graphite, B) the schematic representation of lithium intercalation in the regenerated graphite, and C) the rate performance of the regenerated graphite (Reproduced with permission.[75] Copyright 2023, The Authors). D) Schematic of the regeneration process of S-LCO and HAADF-STEM images of both S-LCO and R-LCO and the corresponding FFT patterns of the marked regions (Reproduced with permission.[20] Copyright 2023, American Chemical Society).

SEI layer on graphite particles to a compact and mostly inorganic one with a thickness of 30 nm (Figure 4B), but allowed the retaining of volatile active lithium in graphite interlayer. By taking advantage of the reconstructed SEI and residual active lithium, the regenerated electrodes delivered a high initial Coulombic efficiency of 104.7% without any prelithiation treatment. Chen et al. applied selective Joule heating for only seconds to efficiently decompose the resistive impurities of spent graphite.[74] The pulsed current, temperature, and time are shown in Figure 4C,D. The recycling process is illustrated in Figure 4E. The pulsed current brought the anode waste to a temperature of ≈2850 K, leading to the decomposition of the SEI, polymer binder, and intercalated molecules together with the formation of a close-contact carbon coating, while retaining the morphology of graphite particles. The graphite with the reconstructed SEI exhibited high initial specific capacity, superior rate performance, and cycling stability.

Except for the SEI, there are numerous defects on the surface of the graphite particles after cycling, such as oxidation of the graphite surface layers. Considering these intrinsic characteristics of degraded graphite, Cheng et al.[75] proposed a strategy based on defect-driven targeted nucleation of metallic tin to repair the surface defect structure of degraded graphite, achieving the regeneration of its electrochemical performances (**Figure** 5A). Such a high temperature not only induced rapid reduction of $SnCl_2$, but also in-situ generated Sn in molten or even vaporous state instantaneously. Since there is a large bonding energy between the carbon atom vacancies and metal atoms according to theoretical calculations, the molten metallic tin nucleated precisely on these defective areas after RHT treatment (1600 °C, 50 ms), achieving targeted regeneration of spent graphite. The heating and cooling rates are as high as 10^3–10^4 °C s^{-1}, which are also key factors for the uniform deposition of Sn nanoparticles. Besides, the number and diameter of Sn particles visibly decreased as the heating temperature increased due to the increasing evaporation, suggesting the necessity of an ultra-short heating time. Interestingly, compared to commercial graphite (CG), the platform capacity of regenerated graphite is much higher. The additional capacity of regenerated graphite originating from its slope region indicated that the extra capacity was contributed by the adsorption at the defect sites (as shown in Figure 5B). As a result, the regenerated graphite showed an enhanced capacity of 458 mAh g^{-1} at 0.2 A g^{-1} and an outstanding rate performance (256.0 mAh g^{-1}) in Figure 5C. In terms of the cathode active materials, Yin et al. presented an efficient, one-step, non-destructive method for regenerating spent $LiCoO_2$ (S-LCO) cathodes within 8 s at 1440 K, as shown in Figure 5D.[20] High-angle annular dark-field scanning transmission electron microscopy

(HAADF-STEM) images of S-LCO, captured at various magnifications and regions, reveal the presence of both spinel phase and layered structure, as confirmed by the associated fast Fourier transform (FFT) analysis. After the RHT process, the regenerated LCO (R-LCO) samples exclusively display an ordered layered structure, as evidenced by the FFT patterns obtained from different areas within the STEM-HAADF images of R-LCO. The capacity of the half-cell assembled with R-LCO and Li metal anode is 133.0 mAh g^{-1} at 0.1 C, which outperforms the furnace-repaired sample. It also shows an enhanced cycle performance and superior rate capacity.

3.2.2. Interphase Repairing

In addition to surface failures, degraded active materials typically exhibit a multitude of bulk defects, such as transition metal dissolution and lithium atom vacancies.[76,77] These defects can trigger phase precipitation inside the material and concurrently lead to the emergence of interphases.[78] Atoms at the interphase are typically in a high energy state and possess a high reactive activity, inducing the formation of chemical bonds and rearrangement of the lattice structure for healing the degraded structure efficiently. When employing RHT for the regeneration of degraded materials, the regenerated ones with new metastable/intermediate structures are preferred because of the short heating time and extremely fast cooling rate.[25] For example, Luo et al. reported an ultrafast conversion strategy of the spent graphite to defect-rich recycled graphite at 1500 °C for 60 s (**Figure 6A**).[79] Taking advantage of the low activation energy associated with structural defects, the high temperature of 1500 °C facilitated the restoration of the layered structure. However, due to the significantly shorter heating duration of 60 s as compared to the 8 hours required for conventional annealing, some defects were retained, benefiting a fast Li^+ diffusion. The defect-rich recycled graphite delivered a good high-rate performance (323 mAh g^{-1} at 2 C), which outperforms commercial graphite (120 mAh g^{-1} at 2 C). Zheng et al. presented an efficient, low-cost, and ultrafast regeneration strategy for rapid regeneration of the spent LFP in only 20 s at 800 °C through RHT (Figure 6B).[19] Lithium acetate and sucrose were used as a lithium replenisher and reducing agent, respectively. As a result, the surface distortion structure of spent LFP was well repaired due to the replenishment of lithium- ion under a high- temperature reductive condition. The regenerated LFP demonstrated an excellent initial capacity of 152 mAh g^{-1} at 0.1 C, a good rate performance, and long-cycling stability (400 cycles at 2 C).

Furthermore, Guo et al.[41] revealed the regeneration mechanism of degraded LFP through atomistic observation. The Li/Fe antisites were efficiently reordered by RHT within several seconds. According to the simulation, the reordering of LiFe antisite defects was composed of two primary steps: the first step was the reordering of Li from the Fe site to its original Li site (0.91 eV) and the second step was the return of Fe in Fe/Li to its original Fe site (0.19 eV). For spent LFP with plenty of Li vacancies (Li vacancies), the energy barrier for Fe migration and Fe/Li reordering was up to 1.12 eV (Figure 6C). After lithiation, the reduction in Li vacancies lowered the energy barrier of Fe/Li reordering to 0.19 eV. In contrast to the goal of completely eradicating defects, Luo et al. controllably introduced the Li-Fe antisite defects and a 2D tensile strain into the lattice of LFP by an ultrafast nonequilibrium high-temperature shock technology.[80] In the nonequilibrium HTS heating process, a number of Li–Fe antisite defects and lattice strain were generated and preserved in the subsequent short-term calcination and cooling process. Experimental evidence and kinetic analysis showed that Li-Fe antisite defects provided a new 2D Li^+ isotropic diffusion channel different from [010] (1D anisotropic diffusion), and the tensile strain field reduced the energy barrier of the new 2D diffusion path. The unique multiscale coupling structure of Li-Fe antisite defects and lattice strain achieved 2D diffusion and effectively reduced the energy barrier of Li^+ diffusion in the electrochemical process, leading to excellent superior electrochemical properties (high-capacity retention of 84.4% after 2000 cycles at 10 C).

4. Valuable Metal Elements Reutilization

Although the element recovery methods based on pyrometallurgy and hydrometallurgy have the problems of high energy consumption and heavy pollution, their technical solutions are mature and still widely adopted by most battery recycling companies, such as GEM in China, Retriev Technologies in America, and Umicore in Belgium.[2] Therefore, further improving the leaching kinetics and selectivity of metal elements is crucial to reducing recycling costs and improving recycling efficiency, which will help promote the transformation of traditional hydrometallurgical technology to new and efficient hydrometallurgical technology. Zhu et al.[40] reported a reducing strategy for $LiNi_{0.3}Co_{0.2}Mn_{0.5}O_2$ (NCM325) cathode materials through RHT with uniform temperature distribution, high heating and cooling rates (≈10^4 °C s^{-1}), high temperatures (up to ≈2200 °C), and ultrafast reaction times (≈20 s). Such a high temperature decomposed the active cathode materials into metals or metal oxides with the assistant of carbon reduction effects. Considering the large vapor pressure, the Li_2O evaporated preferentially from the inside of the calcined products and then recrystallized on the surface due to the ultrafast heating/cooling rate and short reaction duration, making the selective leaching by water possible. As shown in **Figure 7A**, lithium ions can be selectively leached through water leaching after the carbothermal shock process with an efficiency of >90%. Ni, Co, and Mn were recovered by dilute acid leaching with efficiencies >98%. Chen et al.[45] heated the black mass via RHT to >2100 K within seconds, leading to a ≈1000-fold increase in subsequent leaching kinetics (Figure 7B). All of the battery metals showed high recovery yields, regardless of their chemistries and the cell history, using even diluted acids like 0.01 M HCl.

Remanufacturing metal salt precursors to obtain active materials for lithium-ion batteries is one of the important ways to recycle key metal resources. However, traditional heating methods require a long-time (usually several hours) heat treatment to produce fine crystalline structures that take place in a complicated reaction process with a low heating rate and sluggish reaction kinetics, leading to high energy consumption, large carbon emissions, and low manufacturing efficiency. To address these challenges, RHT synthesis strategies were proposed. Using metal salts as precursors, Zhu et al.[81] successfully synthesized various cathode materials through RHT (Figure 7C)

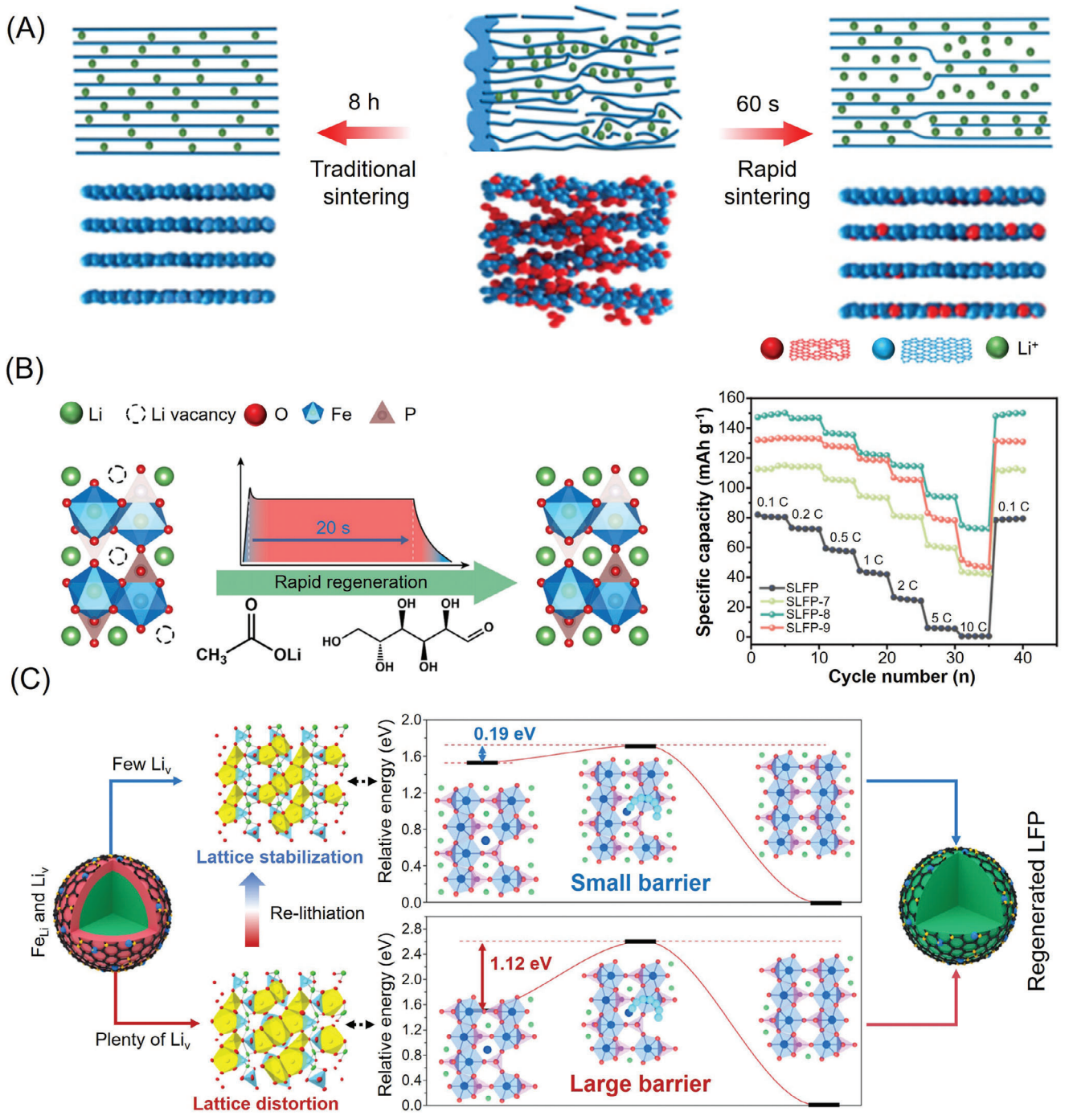

Figure 6. Interphase reparation. A) The schematic diagram for the regeneration process of degraded graphite (Reproduced with permission.[79] Copyright 2022, Tsinghua University Press), B) rapid regeneration of degraded LFP via RHT (Reproduced with permission.[19] Copyright 2023, Elsevier), and C) mechanism of reordering antisite Li/Fe defects (Reproduced with permission.[41] Copyright 2024, The Royal Society of Chemistry).

including $LiMn_2O_4$, $LiCoO_2$, $LiFePO_4$, and Li-rich-layered oxide/NiO heterostructure materials. The ultrahigh heating rate and a nonequilibrium reaction process enabled a fast reaction kinetics and a precise one-step formation process of cathode materials within a few seconds, avoiding complicated multistep reactions in the traditional synthesis methods with a low heating rate.

Despite the LIBs, as one of the most promising energy storage devices, zinc-air batteries need the ORR/OER in the cathode side, which calls for low-cost bifunctional catalysts as cathode materials. Thus, Jiao et al.[32] prepared NiMnCo-activated carbon (NiMnCo-AC) catalysts from spent $LiNi_{1-x-y}Mn_xCo_yO_2$ cathodes efficiently through a rapid thermal radiation method. The rapid thermal radiation process induced the formation of

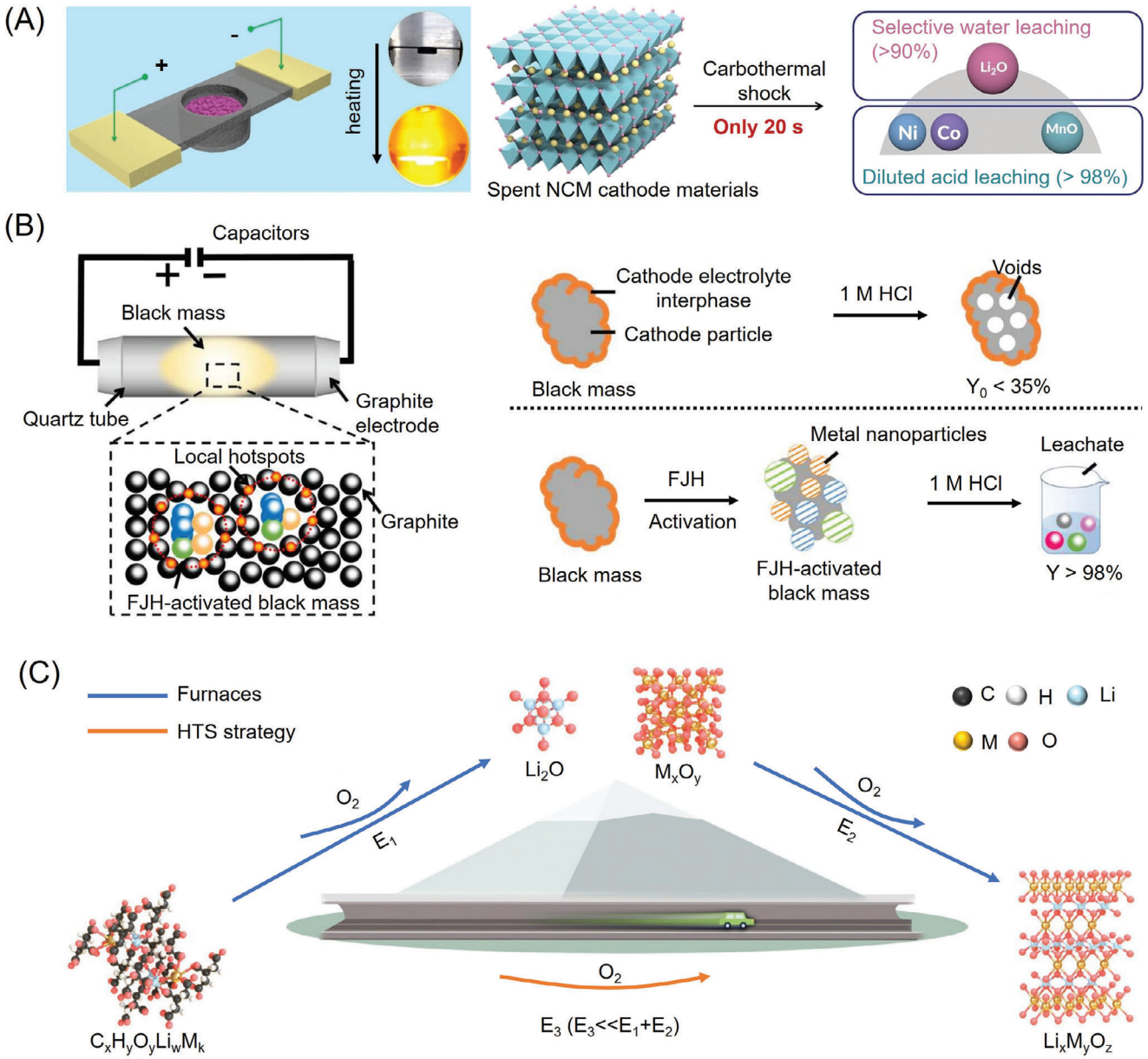

Figure 7. RHT-assisted hydrometallurgical recycling of valuable metal elements. A) prior extraction of lithium from degraded NCM (Reproduced with permission.[40] Copyright 2023, Wiley), B) enhanced leaching rate of cathode materials (Reproduced with permission.[45] Copyright 2023, The Authors), and C) efficient preparation of cathode materials using metal salt precursors for LIBs (Reproduced with permission.[81] Copyright 2022, Wiley).

NiMnCo nanoparticles, while the limited heating time prevented the nanoparticles from growing. The obtained NiMnCo nanoparticles are two phases coexisting, including metallic Ni in the core and spinel $NiMnCoO_4$ in the shell, presenting high electrocatalytic activity to both ORR and OER. Zhu et al.[82] applied a high-temperature shock method to transform spent cathode materials ($LiCoO_2$ and $LiMn_2O_4$) into Co-MnO bifunctional catalyst for Li-S batteries. Owing to the synergistic catalytic and anchoring effect of polysulfide species, the S/Co-MnO@CF cathode exhibits excellent rate performance (707 mAh g^{-1} at 4 C) and high cycling stability (capacity fading of 0.058% per cycle over 400 cycles at 1 C) under a low areal catalyst loading (<0.5 wt%). Yang et al.[83] devised an ultra-fast (15 s), efficient, and universal strategy to synthesize multiple components of spinel oxide (Co_3O_4-JH, Mn_3O_4-JH, $CoMn_2O_4$-JH, and $CoFe_2O_4$-JH) as oxygen reduction catalysts. The oxygen content and particle size of the target products could be regulated by reasonable control of reaction conditions, which provides a feasible way to obtain defective oxide nanoparticles.

5. Scale-Up of RHT

RTH is promising to be easily scaled up in the way of flow-type shock heating, which is compatible with existing industrial

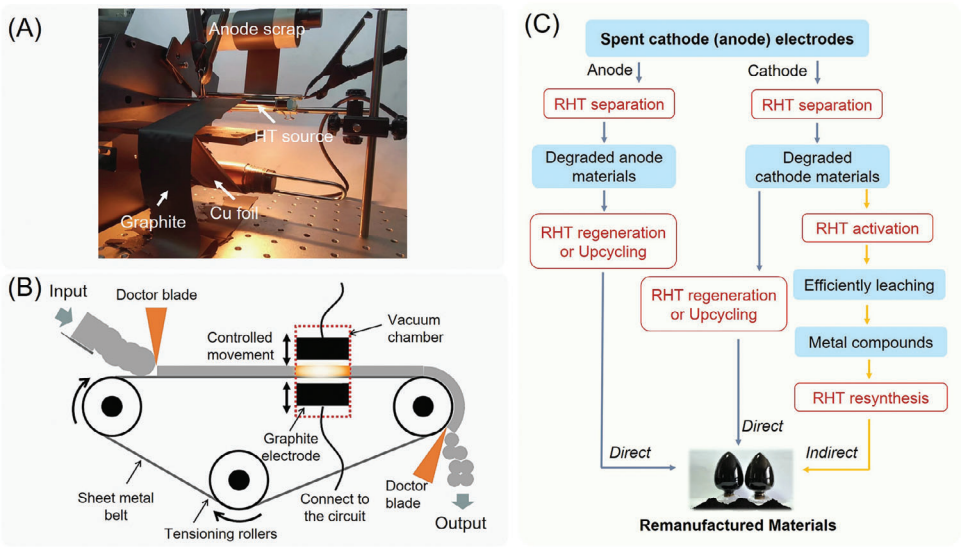

Figure 8. Scale-up mode: A) a picture of the automatic roll-to-roll setup for the anode scrap separation based on RHT (Reproduced with permission.[31] Copyright 2023, The Royal Society of Chemistry), B) conceptual design of a continuous RHT reactor (Reproduced with permission.[45] Copyright 2023, The Authors), and (C) flow diagram of the close-loop recycling of spent electrodes based on RHT.

production. Moreover, both self-heating and shock-type heating methods can be adapted into the flow-type shock heating process to facilitate scaling up. Although research on RHT is primarily confined to the laboratory scale at present, there are already some preliminary indications for its potential scale-up in production.

As depicted in **Figure** 8A, the anode scrap tape was released at a rate of 5 m min^{-1} passing through the heater and mechanical stress section, allowing the graphite to fall into a collector continuously and spontaneously.[31] Within this setup, samples experience a rapid temperature increase due to the exposure to a closed, high-temperature heater. This equipment is well-suited for the continuous processing of film samples like electrode scraps that are generated in industrial manufacturing. Furthermore, powder samples, particularly those with high resistance, can be conveyed through the high-temperature zone on a heat-resistant belt for rapid high-temperature treatment. Concurrently, for conductive powder materials, the rapid high-temperature processing can also be achieved through self-heating mechanisms. As shown in Figure 8B, utilizing positive and negative graphite electrodes, the current is directly conducted through the powder on the conveyor belt.[45] This process leverages the resistance of the conductive powder layer to produce Joule heat. In conjunction with the movement of the conveyor belt, this method enables the continuous, large-scale, and swift high-temperature treatment of the powder. Beyond these accomplishments, scaling up RHT is still confronted with considerable challenges, including the critical need for advanced heaters, the high cost of electricity, and the substantial capital investment required for electrothermal systems.[84] Especially, the design of the heater of RHT instrument presents a significant challenge in the engineering of RHT equipment. In order to ensure the accuracy, controllability, stability, and uniformity of temperature, heater needs to have a high melting point to resist melting or evaporation, stable mechanical properties to resist abrasion or distortion, and stable chemical properties to resist oxidation or reduction at high temperatures. Besides, considering the differences in heat dissipation rates along different directions (for example, the parts in contact with electrodes dissipate heat faster), the shape of the heater should be rationally designed for the uniformity of temperature.

Considering that closed-loop recycling involves a combination of various technologies, the scaling up of RHT recycling technology depends not only on automated equipment but also on a viable process route. According to the above content, the RHT is showing excellent flexibility in reusing both spent cathodes and anodes toward a circular economy instead of a resource-based economy. The recycling flow diagram based on RHT is rationally designed in Figure 8C including anode direct recycling, cathode direct recycling, and cathode indirect recycling. Although no closed-loop recycling route based on RHT has been commercialized to date, the recycling technology based on RHT has been developed rapidly and has shown good results at various recycling nodes since its first report by Hu et al.[85] in 2018. The combination of RHT with existing mature hydrometallurgical recycling processes is an important modified process route, expected to be the earliest to realize the commercialization of RHT recycling technology. Additionally, considering that graphite is the mainstream anode material with both a simple composition and stable structure, its direct recycling route based on RHT is also expected to achieve commercialization quickly. In contrast, the cathode materials are complex and diverse in composition and structure. The commercialization process of RHT recycling is still full of challenges. Therefore, the automatic equipment and viable recycling routes for the real scale-up application of RHT are both necessary and remain in further development.

6. Environmental and Economic Benefits

In industrial development, the environmental and economic benefits of battery recycling technologies are the key indicators for evaluating its business value.[86] Moreover, the economic

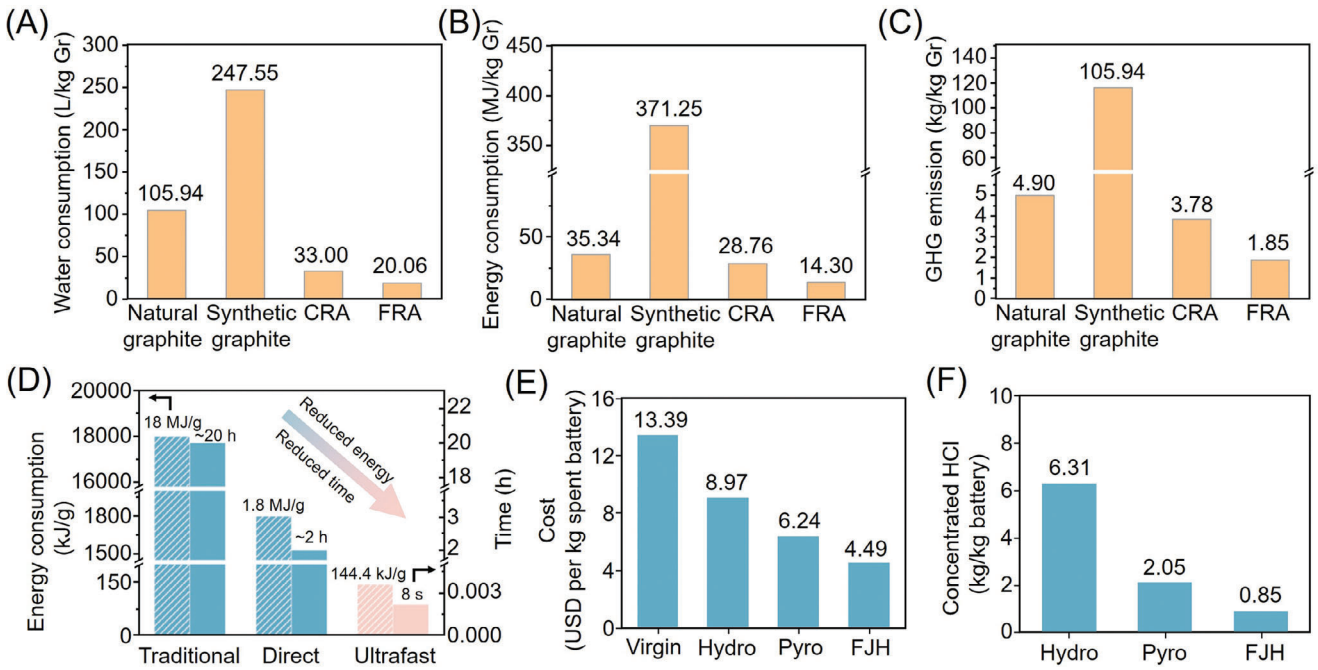

Figure 9. Economic and environmental analysis of the RHT recycling process. A) The water consumption, B) energy consumption, and C) greenhouse gas emission (GHG) in producing 1 kg of graphite anode materials (Reproduced with permission.[74] Copyright 2022, Wiley); D) energy consumption and operation times of different regeneration processes (Reproduced with permission.[20] Copyright 2023, American Chemical Society); E) cost analysis and F) concentrated 12 M HCl consumption in treating 1 kg of spent batteries (Reproduced with permission.[45] Copyright 2023, The Authors). (Notes: the "FRA," "FJH," and "Ultrafast" represent the RHT recycling.).

benefits of battery recycling are closely related to environmental protection. Recycling of spent lithium-ion batteries helps to address the shortage of natural mineral resources, avoid potential environmental hazards, and promote sustainable development. Compared with pyrometallurgy and hydrometallurgy methods, recycling methods based on RHT not only produce active materials with recovered or even upgraded battery performances but also increase environmental and economic benefits. GREET 2020 and EverBatt 2020 software packages are often utilized for the life cycle analysis.[87,88] For the separation of active materials, in contrast to previously burned or discarded graphite, RHT recycling has significantly lower energy and carbon footprint (≈50X reduction), near-zero waste generation, making graphite recycling available, economical, and profitable (4.84 \$ kg^{-1} anode).[31] Besides, the regeneration of the degraded graphite through RHT also presents a huge reduction in recycling cost by ≈85%, greenhouse emission by ≈98%, water use by ≈92%, and energy use by ≈96% compared with the synthetic graphite production method (**Figure** 9A–C).[74] Taking LCO as an example, the RHT regeneration process also exhibits significantly less operating time and energy consumption compared with the traditional metallurgical processes and direct repair process based on furnace heating (Figure 9D).[20] Furthermore, the RHT-assisted hydrometallurgy recycling methods can significantly reduce materials input, particularly leading to a decrease in recycling cost and wastewater emission (Figure 9E,F).[45] Therefore, this analysis highlights that RHT recycling has higher environmental and economic benefits over traditional recycling methods including pyrometallurgy, hydrometallurgy, and furnace heating-based recycling processes.

7. Conclusion and Perspective

The goal of green recycling for failed lithium-ion batteries is to address the scarcity of natural mineral resources and to mitigate potential environmental risks. This is essential for fostering the sustainable growth of the lithium-ion battery sector. As detailed in **Table** 1, RHT, characterized by its rapid heating/cooling rates, high temperatures, and short processing times, offers a highly efficient, low-carbon, cost-effective, and profitable method for recycling and reusing the active materials of LIBs.

In this review, we first discuss the various rapid heating methods. Then, we explore the material recycling strategies enabled by RHT, which include the precise separation of degraded active materials from current collectors and the regeneration of these degraded materials. Given the spatially confined nature of failure mechanisms in degraded active materials (where failure regions are typically found at surfaces, interfaces, or interphases), we summarize the regulatory principles of the rapid heating method. Finally, focusing on the current mainstream element recycling strategies in the industry, hydrometallurgical and pyrometallurgical recycling, we introduce the research progress of RHT in enhancing the leaching efficiency of metal elements and in energy-saving remanufacturing. As concluded in **Figure** 10, leveraging its fast and finely controllable kinetics, RHT holds great promise for spent battery recycling applications in separation, regeneration, and remanufacturing.

Although a series of research results have been achieved compared to traditional hydrometallurgy and pyrometallurgy, which are based on an element recycling strategy, RHT, which is based

Table 1. Detail information of various RHT methods reported in literature.

Temperature	Time	Heating rate	Application	Refs.
1500 °C	1 s	$\approx 10^3$ °C s^{-1}	Active materials separation	[31]
1900 K	150 ms	$\approx 10^4$ °C s^{-1}	SEI reconstruction	[73]
2850 K	≈100 ms	$\approx 10^5$ °C s^{-1}	Spent graphite regeneration	[74]
1600 °C	50 ms	$\approx 10^4$ °C s^{-1}	Spent graphite upcycling	[75]
1440 K	8 s	$\approx 10^3$ °C s^{-1}	Spent $LiCoO_2$ regeneration	[20]
1500 °C	60 s	$\approx 10^3$ °C s^{-1}	Spent graphite upcycling	[79]
800 °C	20 s	$\approx 10^3$ °C s^{-1}	Spent $LiFePO_4$ regeneration	[19]
1260 °C	1 s	$\approx 10^3$ °C s^{-1}	Spent $LiFePO_4$ regeneration	[41]
2200 °C	20 s	$\approx 10^4$ °C s^{-1}	Spent NCM325 reduction	[40]
2120 K	110 ms	$\approx 10^4$ °C s^{-1}	Battery metal recycling	[45]
660 °C	9 s	$\approx 10^3$ °C s^{-1}	Cathode material synthesis	[81]
650 °C	15 s	$\approx 10^2$ °C s^{-1}	Nanocrystalline spinel oxides synthesis	[83]

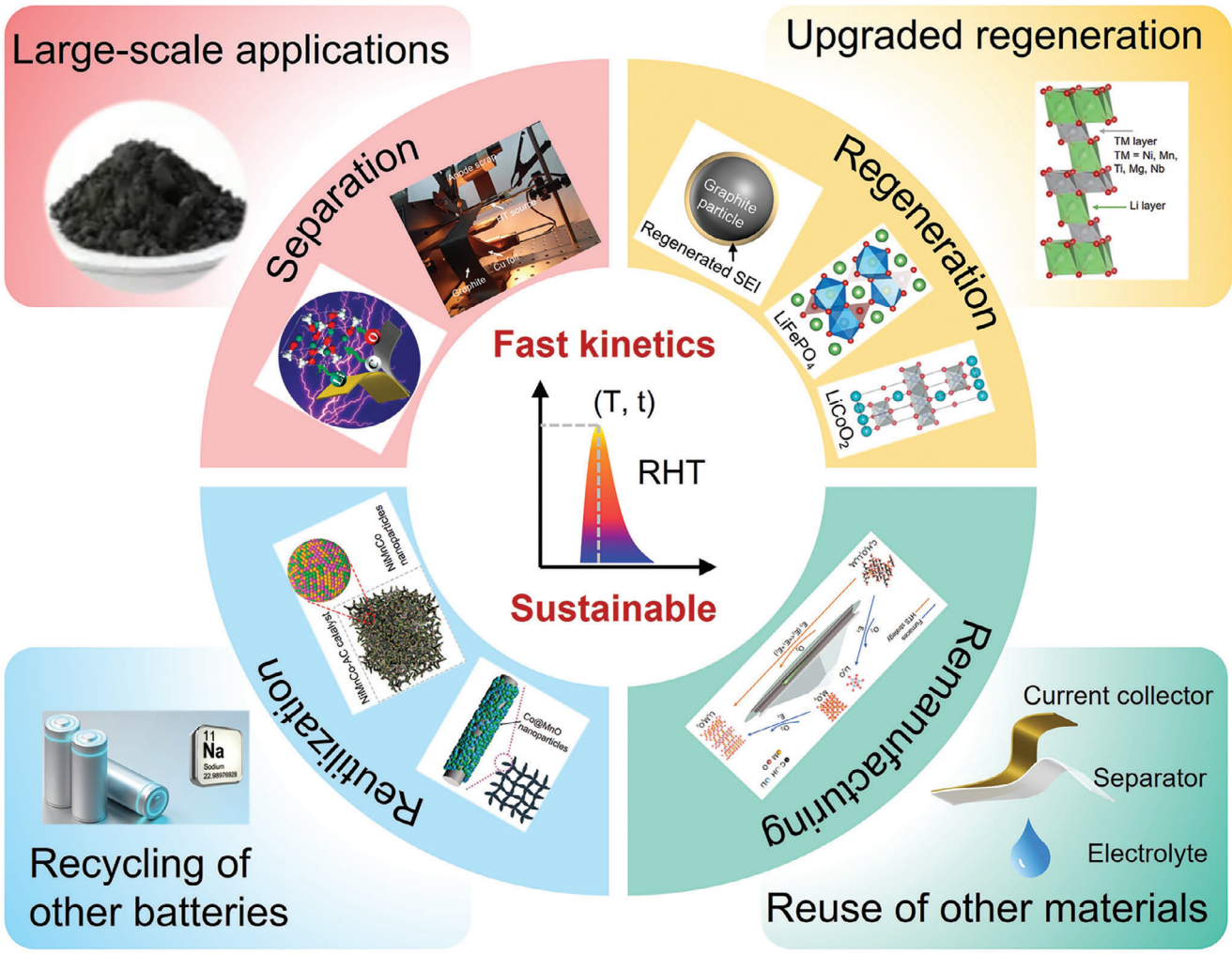

Figure 10. Conclusions and perspectives of RHT for the recycling of lithium-ion batteries. Reproduced with permission.[31] Copyright 2023, The Royal Society of Chemistry. Reproduced with permission.[59] Copyright 2021, Elsevier. Reproduced with permission.[32] Copyright 2022, the Authors. Reproduced with permission.[82] Copyright 2024, Wiley. Reproduced with permission.[81] Copyright 2022, Wiley. Reproduced with permission.[19] Copyright 2023, Elsevier. Reproduced with permission.[20] Copyright 2023, American Chemical Society.

on a material recycling strategy, is still in its infancy. There is still a significant amount of room for exploration in the complex and ever-changing battery material system. The important research directions are as follows:

1) When reusing the spent battery materials based on RHT, it is difficult for us to find the best reaction parameters in just one attempt. The parameter adjustment range for RHT is quite large, and determining reaction parameters (heating temperature, heating time, number of heating cycles, and heating and cooling rates, etc.) requires a certain amount of time investment. Therefore, we need to introduce artificial intelligence, machine learning, and other methods to improve the efficiency of determining reaction parameters.
2) The degraded materials reported in the literature often come from only one or the same type of battery. However, for large-scale applications, degraded active materials will be quite different in morphology and size—even if the main components are similar, such as LFP, NCM, or graphite—and in various failure states, such as different lithium contents. The consistent regeneration or upgraded regeneration of mixed degraded active materials is crucial for their electrochemical performance. To address this challenge, it has been reported that screening of spent batteries could be a potentially efficient method to reduce the difference of degraded active materials according to the physical attributes (such as size, weight, and shape), chemical composition (like metal content), or electronic properties (such as voltage and resistance) of used batteries.[89] This facilitates the precise RHT treatment of separated degraded active materials, which is conducive to their consistent and effective restoration. Additionally, for the occurrence of various failure mechanisms (e.g., cracking, lithium vacancy, and lithium-nickel intermixing, lithium-iron antisites), it might be difficult to repair the multiple failure states by one-shock RHT. Fortunately, the RHT method offers dynamic temperature modulation with a fine time and temperature resolution and unique programmability, providing an opportunity to repair the spent cathode materials with multiple failure mechanisms through a rational designed multistep RHT process.
3) Generally, degraded active materials are from batteries produced 5–10 years ago and lag current commercial ones in terms of capacity, rate, etc. Therefore, regenerated active materials that only restore the structure and composition are difficult to satisfy current and future applications. It is necessary to up-manufacture them according to the development direction of active materials. To date, due to the extreme high-temperature thermodynamics and ultrafast kinetics of RHT, several advanced cathode materials, including single-crystal NCM cathodes,[90] high-entropy cathodes,[91] and surface-modified active materials,[92] have been successfully synthesized from metallic compound precursors via RHT. However, there remains a scarcity of experience in upgrading active materials derived from spent sources.
4) In addition to the valuable cathode and anode active materials, due to the huge volume of LIBs, the recycling and reuse of other materials (such as electrolytes, separators, current collectors, etc.) are also of great significance to the sustainability of LIBs. Notably, sodium-ion batteries, solid–state lithium batteries, and lithium metal batteries are very promising for next-generation energy storage applications. Considering that they have similar structures and compositions to LIBs, the experience and strategies gained from RHT recycling of LIBs can be transferred and applied to their recycling in parallel.

Acknowledgements

H.Z. and Y.S. contributed equally to this work. The authors acknowledge the financial support from the Key R&D Program of Hubei Province (2024BCB091), the Natural Science Foundation of Hubei Province (2022CFA031), and the Interdisciplinary Research Program of HUST (2023JCYJ004).

Conflict of Interest

The authors declare no conflict of interest.

Keywords

battery recycling, defects and interfaces, rapid heating, sustainability

Received: October 18, 2024
Revised: December 2, 2024
Published online:

[1] D. Castelvecchi, *Nature* **2021**, *596*, 336.
[2] E. Fan, L. Li, Z. Wang, J. Lin, Y. Huang, Y. Yao, R. Chen, F. Wu, *Chem. Rev.* **2020**, *120*, 7020.
[3] X. Zhang, L. Li, E. Fan, Q. Xue, Y. Bian, F. Wu, R. Chen, *Chem. Soc. Rev.* **2018**, *47*, 7239.
[4] J. Baars, T. Domenech, R. Bleischwitz, H. E. Melin, O. Heidrich, *Nat. Sustain.* **2021**, *4*, 71.
[5] X. Xiao, L. Wang, Y. Wu, Y. Song, Z. Chen, X. He, *Energy Environ. Sci.* **2023**, *16*, 2856.
[6] G. Harper, R. Sommerville, E. Kendrick, L. Driscoll, P. Slater, R. Stolkin, A. Walton, P. Christensen, O. Heidrich, S. Lambert, A. Abbott, K. Ryder, L. Gaines, P. Anderson, *Nature* **2019**, *575*, 75.
[7] M. Chen, X. Ma, B. Chen, R. Arsenault, P. Karlson, N. Simon, Y. Wang, *Joule* **2019**, *3*, 2622.
[8] K. Du, E. H. Ang, X. Wu, Y. Liu, *Energy Environ. Mater.* **2022**, *5*, 1012.
[9] J. Wang, K. Jia, J. Ma, Z. Liang, Z. Zhuang, Y. Zhao, B. Li, G. Zhou, H.-M. Cheng, *Nat. Sustain.* **2023**, *6*, 797.
[10] S. Natarajan, V. Aravindan, *Adv. Energy Mater.* **2018**, *8*, 1.
[11] K. Jia, G. R. Yang, Y. J. He, Z. J. Cao, J. T. Gao, H. Y. Zhao, Z. H. Piao, J. X. Wang, A. M. Abdelkader, Z. Liang, R. V. Kumar, G. M. Zhou, S. J. Ding, K. Xi, *Adv. Mater.* **2024**, *36*, 2313273.
[12] C. R. Birkl, M. R. Roberts, E. McTurk, P. G. Bruce, D. A. Howey, *J. Power Sources* **2017**, *341*, 373.
[13] W. Cai, Y. X. Yao, G. L. Zhu, C. Yan, L. L. Jiang, C. He, J. Q. Huang, Q. Zhang, *Chem. Soc. Rev.* **2020**, *49*, 3806.
[14] M. Gu, A. M. Rao, J. Zhou, B. Lu, *Energy Environ. Sci.* **2023**, *16*, 1166.
[15] Y. Shi, M. Zhang, Y. S. Meng, Z. Chen, *Adv. Energy Mater.* **2019**, *9*, 1900454.
[16] P. P. Xu, Q. Dai, H. P. Gao, H. D. Liu, M. H. Zhang, M. Q. Li, Y. Chen, K. An, Y. S. Meng, P. Liu, Y. R. Li, J. S. Spangenberger, L. Gaines, J. Lu, Z. Chen, *Joule* **2020**, *4*, 2609.
[17] Y. Q. Guo, X. B. Liao, P. J. Huang, P. Lou, Y. Q. Su, X. F. Hong, Q. G. Han, R. H. Yu, Y. C. Cao, S. J. Chen, *Energy Storage Mater.* **2021**, *43*, 348.

[18] X. Ma, M. Chen, Z. Zheng, D. Bullen, J. Wang, C. Harrison, E. Gratz, Y. Lin, Z. Yang, Y. Zhang, F. Wang, D. Robertson, S.-B. Son, I. Bloom, J. Wen, M. Ge, X. Xiao, W.-K. Lee, M. Tang, Q. Wang, J. Fu, Y. Zhang, B. C. Sousa, R. Arsenault, P. Karlson, N. Simon, Y. Wang, *Joule* **2021**, *5*, 2955.
[19] S.-H. Zheng, X.-T. Wang, Z.-Y. Gu, H.-Y. Lü, X.-Y. Zhang, J.-M. Cao, J.-Z. Guo, X.-T. Deng, Z.-T. Wu, R.-H. Zeng, X.-L. Wu, *J. Power Sources* **2023**, *587*, 233679.
[20] Y.-C. Yin, C. Li, X. Hu, D. Zuo, L. Yang, L. Zhou, J. Yang, J. Wan, *ACS Energy Lett.* **2023**, *8*, 3005.
[21] T. Y. Li, L. Tao, L. Xu, T. T. Meng, B. C. Clifford, S. K. Li, X. P. Zhao, J. C. Rao, F. Lin, L. B. Hu, *Adv. Funct. Mater.* **2023**, *33*, 2302951.
[22] Y. Dong, Y. Rao, H. Liu, H. Zhang, R. Hu, Y. Chen, Y. Yao, H. Yang, *eScience* **2024**, *4*, 100253
[23] H. Zhang, Q. Ouyang, L. Yu, R. Hu, J. Wan, B. Song, Q. Huang, Y. Yao, *Adv. Funct. Mater.* **2023**, *33*, 2301375.
[24] Y. J. Mei, J. L. Chen, Q. Wang, Y. Q. Guo, H. W. Liu, W. H. Shi, C. Lin, Y. F. Yuan, Y. H. Wang, B. Y. Xia, Y. G. Yao, *Sci. Adv.* **2024**, *10*, adq6758.
[25] Y.-C. Han, P.-Y. Cao, Z.-Q. Tian, *Acc. Mater. Res.* **2023**, *4*, 648.
[26] S. M. Dou, J. Xu, X. Y. Cui, W. D. Liu, Z. C. Zhang, Y. D. Deng, W. B. Hu, Y. N. Chen, *Adv. Energy Mater.* **2020**, *10*, 2001331.
[27] C. W. Wang, W. W. Ping, Q. Bai, H. C. Cui, R. Hensleigh, R. L. Wang, A. H. Brozena, Z. P. Xu, J. Q. Dai, Y. Pei, C. L. Zheng, G. Pastel, J. L. Gao, X. Z. Wang, H. Wang, J. C. Zhao, B. Yang, X. Y. Zheng, J. Luo, Y. F. Mo, B. Dunn, L. B. Hu, *Science* **2020**, *368*, 521.
[28] W. W. Ping, C. W. Wang, R. L. Wang, Q. Dong, Z. W. Lin, A. H. Brozena, J. Q. Dai, J. Luo, L. B. Hu, *Sci. Adv.* **2020**, *6*, abc8641.
[29] X. Yao, S. Chen, C. Wang, T. Chen, J. Li, S. Xue, Z. Deng, W. Zhao, B. Nan, Y. Zhao, K. Yang, Y. Song, F. Pan, L. Yang, X. Sun, *Adv. Energy Mater.* **2023**, *14*, 2303422.
[30] X. K. Pang, Y. X. Mao, F. Q. Mao, M. Liu, Y. H. Zhao, P. Xu, X. Wang, X. Zhan, F. Wang, L. Zhang, *J. Phys. Chem. C* **2024**, *128*, 14127.
[31] H. Zhang, Y. Ji, Y. Yao, L. Qie, Z. Cheng, Z. Ma, X. Qian, R. Yang, C. Li, Y. Guo, Y. Yuan, H. Xiao, H. Yang, J. Ma, J. Lu, Y. Huang, *Energy Environ. Sci.* **2023**, *16*, 2561.
[32] M. L. Jiao, Q. Zhang, C. L. Ye, Z. B. Liu, X. W. Zhong, J. X. Wang, C. Li, L. X. Dai, G. M. Zhou, H. M. Cheng, *Proc. Nat. Acad. Sci. USA* **2022**, *119*, 2202202119.
[33] Z. Wu, M. Fan, H. Jiang, J. Dai, K. Liu, R. Hu, S. Qin, W. Xu, Y. Yao, J. Wan, *Angew. Chem., Int. Ed. n/a(n/a)*, e202413932.
[34] Y. Li, X. Liu, T. Wu, X. Zhang, H. Han, X. Liu, Y. Chen, Z. Tang, Z. Liu, Y. Zhang, H. Liu, L. Zhao, D. Ma, W. Zhou, *Nat. Commun.* **2024**, *15*, 5495.
[35] Q. Y. Yin, Q. Liu, Y. T. Liu, Z. B. Qu, F. Sun, C. Z. Wang, X. T. Yuan, Y. Z. Li, L. Shen, C. Zhang, Y. F. Lu, *Adv. Mater.* **2024**, *36*, 2404689.
[36] Q. Liu, B. Lu, F. Nichols, J. Ko, R. Mercado, F. Bridges, S. Chen, *SusMat.* **2022**, *2*, 335.
[37] W. Xiang, R. Ma, X. Liu, X. Kong, S. Shen, L. Wang, Z. Jin, Z. Zhan, C. Chen, C. Wang, *Nano Energy* **2023**, 116.
[38] S. Dong, Y. L. Song, K. Ye, J. Yan, G. L. Wang, K. Zhu, D. X. Cao, *Ecomat* **2022**, *4*, 12212.
[39] Y. M. Mao, P. H. Ma, T. Y. Li, H. Liu, X. P. Zhao, S. F. Liu, X. X. Jia, S. O. Rahaman, X. Z. Wang, M. H. Zhao, G. Chen, H. Xie, A. H. Brozena, B. Zhou, Y. G. Luo, R. Tarte, C. Wei, Q. Wang, R. M. Briber, L. B. Hu, *Nat. Commun.* **2024**, *15*, 3893.
[40] X. H. Zhu, Y. J. Li, M. Q. Gong, R. Mo, S. Y. Luo, X. Yan, S. Yang, *Angew. Chem.-Int. Ed.* **2023**, *135*, 202300074.
[41] Y. Guo, Y. Yao, C. Guo, Y. Song, P. Huang, X. Liao, K. He, H. Zhang, H. Liu, R. Hu, W. Wang, C. Li, S. Wang, A. Nie, Y. Yuan, Y. Huang, *Energy Environ. Sci.* **2024**, *17*, 7749.
[42] D. X. Luong, K. V. Bets, W. A. Algozeeb, M. G. Stanford, C. Kittrell, W. Chen, R. V. Salvatierra, M. Ren, E. A. McHugh, P. A. Advincula, Z. Wang, M. Bhatt, H. Guo, V. Mancevski, R. Shahsavari, B. I. Yakobson, J. M. Tour, *Nature* **2020**, *577*, 647.
[43] K. M. Wyss, W. Y. Chen, J. L. Beckham, P. E. Savas, J. M. Tour, *ACS Nano* **2022**, *16*, 7804.
[44] J. J. Lu, S. L. Liu, J. H. Liu, G. Y. Qian, D. Wang, X. Z. Gong, Y. D. Deng, Y. N. Chen, Z. Wang, *Adv. Energy Mater.* **2021**, *11*, 2102103.
[45] W. Chen, J. Chen, K. V. Bets, K. V. Salvatierrax, K. M. Wyss, G. Gao, C. H. Choi, B. Deng, X. Wang, J. T. Li, N. L. C. Kittrell, L. Eddy, P. Scotland, Y. Cheng, S. Xu, B. Li, M. B. Tomson, Y. Han, B. I. Yakobson, J. M. Tour, *Sci. Adv.* **2023**, *9*, eadh5131.
[46] M. Fan, X. Chang, Q. Meng, L. J. Wan, Y. G. Guo, *SusMat* **2021**, *1*, 241.
[47] S. Kim, J. Bang, J. Yoo, Y. Shin, J. Bae, J. Jeong, K. Kim, P. Dong, K. Kwon, *J. Cleaner Prod.* **2021**, *294*, 126329.
[48] M. Wang, Q. Tan, L. Liu, J. Li, *ACS Sustainable Chem. Eng.* **2019**, *7*, 8287.
[49] Y. Guo, C. Guo, P. Huang, Q. Han, F. Wang, H. Zhang, H. Liu, Y.-C. Cao, Y. Yao, Y. Huang, *eScience* **2023**, *3*, 100091.
[50] Z. Qin, J. Li, T. Zhang, Z. Wen, Z. Zheng, Y. Zhang, N. Zhang, C. Jia, X. Liu, G. Chen, *J. Mater. Chem. A* **2022**, *10*, 23905.
[51] Z. Chen, R. Feng, W. Wang, S. Tu, Y. Hu, X. Wang, R. Zhan, J. Wang, J. Zhao, S. Liu, L. Fu, Y. Sun, *Nat. Commun.* **2023**, *14*, 4648.
[52] Y. Zhao, Y. Kang, M. Fan, T. Li, J. Wozny, Y. Zhou, X. Wang, Y.-L. Chueh, Z. Liang, G. Zhou, J. Wang, N. Tavajohi, F. Kang, B. Li, *Energy Storage Mater.* **2022**, *45*, 1092.
[53] K. K. Halankar, B. P. Mandal, M. K. Jangid, A. Mukhopadhyay, S. S. Meena, R. Acharya, A. K. Tyagi, *RSC Adv.* **2018**, *8*, 1140.
[54] D. Gastol, J. Marshall, E. Cooper, C. Mitchell, D. Burnett, T. Song, R. Sommerville, B. Middleton, M. Crozier, R. Smith, S. Haig, C. R. McElroy, N. van Dijk, P. Croft, V. Goodship, E. Kendrick, *Global Challenges* **2022**, *6*, 2200046.
[55] Y. Yang, G. Huang, S. Xu, Y. He, X. Liu, *Hydrometallurgy* **2016**, *165*, 390.
[56] K. Liu, S. Yang, F. Lai, H. Wang, Y. Huang, F. Zheng, S. Wang, X. Zhang, Q. Li, *ACS Appl. Energy Mater.* **2020**, *3*, 4767.
[57] C. Lei, I. Aldous, J. M. Hartley, D. L. Thompson, S. Scott, R. Hanson, P. A. Anderson, E. Kendrick, R. Sommerville, K. S. Ryder, A. P. Abbott, *Green Chem.* **2021**, *23*, 4710.
[58] X. Chen, S. Li, X. Wu, T. Zhou, H. Ma, *J. Cleaner Prod.* **2020**, *258*, 120943.
[59] C. Yuwen, B. Liu, H. Zhang, S. Tian, L. Zhang, S. Guo, B. Zhou, *J. Cleaner Prod.* **2022**, *333*, 130197.
[60] B. K. Biswal, B. Zhang, M. Thi, P. Tran, J. Zhang, R. Balasubramanian, *Chem. Soc. Rev.* **2024**, *53*, 5552.
[61] C. Lin, A. Tang, H. Mu, W. Wang, C. Wang, *J. Chem.* **2015**, *2015*, 1.
[62] G. Ji, J. Wang, Z. Liang, K. Jia, J. Ma, Z. Zhuang, G. Zhou, H.-M. Cheng, *Nat. Commun.* **2023**, *14*, 584.
[63] Y. Shi, G. Chen, F. Liu, X. Yue, Z. Chen, *ACS Energy Lett.* **2018**, *3*, 1683.
[64] F. Tian, L. B. Ben, H. L. Yu, H. X. Ji, W. W. Zhao, Z. Z. Liu, R. Monteiro, R. M. Ribas, Y. M. Zhu, X. J. Huang, *Nano Energy* **2022**, *98*, 107222.
[65] P. Xu, D. H. S. Tan, B. Jiao, H. Gao, X. Yu, Z. Chen, *Adv. Funct. Mater.* **2023**, *33*, 2213168.
[66] B. Han, Y. Zou, G. Xu, S. Hu, Y. Kang, Y. Qian, J. Wu, X. Ma, J. Yao, T. Li, Z. Zhang, H. Meng, H. Wang, Y. Deng, J. Li, M. Gu, *Energy Environ. Sci.* **2021**, *14*, 4882.
[67] Z. Feng, S. Zhang, X. B. Huang, Y. R. Ren, D. Sun, Y. G. Tang, Q. X. Yan, H. Y. Wang, *Small* **2022**, *18*, 2107346.
[68] N. Takenaka, A. Bouibes, Y. Yamada, M. Nagaoka, A. Yamada, *Adv. Mater.* **2021**, *33*, 2100574.
[69] S. J. An, J. Li, C. Daniel, D. Mohanty, S. Nagpure, D. L. Wood, *Carbon* **2016**, *105*, 52.
[70] H. Adenusi, G. A. Chass, S. Passerini, K. V. Tian, G. H. Chen, *Adv. Energy Mater.* **2023**, *13*, 2203307.
[71] D. Y. Wang, N. N. Sinha, R. Petibon, J. C. Burns, J. R. Dahn, *J. Power Sources* **2014**, *251*, 311.
[72] H. Da, S. Pan, J. Li, J. Huang, X. Yuan, H. Dong, J. Liu, H. Zhang, *Energy Storage Mater.* **2023**, *56*, 457.

[73] Y. S. Ji, H. Zhang, D. Yang, Y. J. Pan, Z. L. Zhu, X. Q. Qi, X. P. Pi, W. C. Du, Z. H. Cheng, Y. G. Yao, L. Qie, Y. H. Huang, *Adv. Mater.* **2024**, *36*, 2312548.
[74] W. Y. Chen, R. V. Salvatierra, J. T. Li, C. Kittrell, J. L. Beckham, K. M. Wyss, N. La, P. E. Savas, C. Ge, P. A. Advincula, P. Scotland, L. Eddy, B. Deng, Z. Yuan, J. M. Tour, *Adv. Mater.* **2023**, *35*, 2207303.
[75] Z. Cheng, Z. Luo, H. Zhang, W. Zhang, W. Gao, Y. Zhang, L. Qie, Y. Yao, Y. Huang, K. K. Fu, *Carbon Energy* **2023**, *6*, e395.
[76] G. T. Park, H. H. Ryu, T. C. Noh, G. C. Kang, Y. K. Sun, *Mater. Today* **2022**, *52*, 9.
[77] Y. Lan, X. Li, G. Zhou, W. Yao, H.-M. Cheng, Y. Tang, *Adv. Sci.* **2024**, *11*, 2304425.
[78] C. Wang, X. Wang, R. Zhang, T. Lei, K. Kisslinger, H. L. Xin, *Nat. Mater.* **2023**, *22*, 235.
[79] J. Luo, J. Zhang, Z. Guo, Z. Liu, S. Dou, W.-D. Liu, Y. Chen, W. Hu, *Nano Res.* **2022**, *16*, 4240.
[80] J. Luo, J. Zhang, Z. Guo, Z. Liu, C. Wang, H. Jiang, J. Zhang, L. Fan, H. Zhu, Y. Xu, R. Liu, J. Ding, Y. Chen, W. Hu, *Adv. Mater.* **2024**, *36*, 2405956.
[81] W. Zhu, J. Zhang, J. Luo, C. Zeng, H. Su, J. Zhang, R. Liu, E. Hu, Y. Liu, W. D. Liu, Y. Chen, W. Hu, Y. Xu, *Adv. Mater.* **2022**, *35*, 2208974.
[82] H. Y. Zhu, S. M. Chen, X. M. Yao, K. Yang, W. G. Zhao, T. W. Chen, L. Y. Yang, F. Pan, *Adv. Funct. Mater.* **2024**, *34*, 2401470.
[83] W. Yang, L. Shang, X. Liu, S. Zhang, H. Li, Z. Yan, J. Chen, *Chin. Chem. Lett.* **2024**, *35*, 109501.
[84] Q. Dong, S. Hu, L. Hu, *Nat. Chem. Eng.* **2024**, *1*, 680.
[85] Y. G. Yao, Z. N. Huang, P. F. Xie, S. D. Lacey, R. J. Jacob, H. Xie, F. J. Chen, A. M. Nie, T. C. Pu, M. Rehwoldt, D. W. Yu, M. R. Zachariah, C. Wang, R. Shahbazian-Yassar, J. Li, L. B. Hu, *Science* **2018**, *359*, 1489.
[86] I. Rey, C. Vallejo, G. Santiago, M. Iturrondobeitia, E. Lizundia, *ACS Sustainable Chem. Eng.* **2021**, *9*, 14488.
[87] Q. Dai, J. Spangenberger, S. Ahmed, L. Gaines, J. C. Kelly, M. Wang, in *Everbatt: A Closed-Loop Battery Recycling Cost and Environmental Impacts Model*, Argonne National Lab.(ANL), Argonne, IL USA **2019**.
[88] M. Wang, A. Elgowainy, U. Lee, A. Bafana, P. T. Benavides, A. Burnham, H. Cai, Q. Dai, U. R. Gracida-Alvarez, T. R. Hawkins, P. V. Jaquez, J. C. Kelly, H. Kwon, Z. Lu, X. Liu, L. Ou, P. Sun, O. Winjobi, H. Xu, E. Yoo, G. G. Zaimes, G. Zang, in *Summary of Expansions and Updates in GREET 2020*, Argonne National Lab. (ANL), Argonne, IL USA **2020**.
[89] S. Tao, H. Liu, C. Sun, H. Ji, G. Ji, Z. Han, R. Gao, J. Ma, R. Ma, Y. Chen, S. Fu, Y. Wang, Y. Sun, Y. Rong, X. Zhang, G. Zhou, H. Sun, *Nat. Commun.* **2023**, *14*, 8032.
[90] H. Huang, L. P. Zhang, H. Y. Tian, J. Q. Yan, J. F. Tong, X. H. Liu, H. X. Zhang, H. Q. Huang, S. M. Hao, J. Gao, L. Yu, H. Li, J. S. Qiu, W. D. Zhou, *Adv. Energy Mater.* **2023**, *13*, 2203188.
[91] C. H. Luan, L. Jiang, X. R. Zheng, Y. H. Cao, Z. Huang, Q. Lu, J. H. Li, Y. Wang, Y. D. Deng, A. L. Rogach, *Chem. Eng. J.* **2023**, *462*, 142180.
[92] D. F. Kong, J. T. Hu, Z. F. Chen, K. P. Song, C. Li, M. Y. Weng, M. F. Li, R. Wang, T. C. Liu, J. J. Liu, M. J. Zhang, Y. G. Xiao, F. Pan, *Adv. Energy Mater.* **2019**, *9*, 1901756.

Hao Zhang is currently working as a lecturer at the School of Materials Science and Engineering, Hubei University. He graduated from University of Science and Technology of China with a doctor's degree in 2018. He did postdoctoral work in Prof. Yao's group at Huazhong University of Science and Technology from 2021 to 2023. His research interest mainly focuses on the direct recycling of spent battery materials.

Yaduo Song is currently a Ph.D. candidate at the School of Materials Science and Engineering, Huazhong University of Science and Technology. She graduated from the University of Electronic Science and Technology of China with a master's degree in 2021. Her research interest mainly focuses on the ultrafast synthesis and rapid direct regeneration of LFP materials.

Yonggang Yao is a Professor in the School of Materials Science and Engineering, Huazhong University of Science and Technology. He obtained his Ph.D. degree at the University of Maryland with Dr. Liangbing Hu. His research mainly focuses on the transient high-temperature synthesis and data-driven material discovery, particularly in the field of energy materials and low-carbon rapid manufacturing.

Yunhui Huang is a Professor in the School of Materials Science and Engineering, Huazhong University of Science and Technology. He received his Ph.D. degree from Peking University. From 2002 to 2004, he worked as an associate professor at Fudan University and as a JSPS fellow at the Tokyo Institute of Technology, Japan. He then conducted postdoctoral research under the mentorship of Mr. John B. Goodenough at the University of Texas at Austin from 2004 to 2007. His research interests include lithium-ion batteries, next-generation batteries, and electrode materials.